ELSEVIER

Earth and Planetary Science Letters 197 (2002) 245–259

EPSL

www.elsevier.com/locate/epsl

Probing Archean lithosphere using the Lu–Hf isotope systematics of peridotite xenoliths from Somerset Island kimberlites, Canada

Stefanie S. Schmidberger [a,b,*], Antonio Simonetti [b], Don Francis [a], Clément Gariépy [b]

[a] *Earth and Planetary Sciences, McGill University, 3450 University Street, Montréal, QC, Canada H3A 2A7*
[b] *GEOTOP, Université du Québec à Montréal, P.O. Box 8888, succ. Centre-Ville, Montréal, QC, Canada H3C 3P8*

Received 6 November 2001; accepted 23 January 2002

Abstract

A knowledge of the Hf isotopic composition of the subcontinental lithosphere beneath Archean cratons is essential to constrain the Hf isotope budget of the Earth's mantle. Hf isotopic measurements were obtained by MC-ICP-MS for a suite of refractory peridotite xenoliths and constituent garnets from the Nikos kimberlite (100 Ma) on Somerset Island in order to constrain the isotopic composition and age of the lithosphere beneath the northern Canadian craton. The low-temperature Nikos peridotites (<1100°C), which represent the shallow Somerset lithosphere, are characterized by higher $^{176}Lu/^{177}Hf$ ratios (0.03–0.05) and Hf isotopic values ($^{176}Hf/^{177}Hf_{(0.1Ga)} = 0.28296$–$0.28419$) than the deep-seated high-temperature peridotites (>1100°C; 0.004–0.03, 0.28265–0.28333, respectively). These differences in Hf isotope signatures suggest that shallow and deep subcontinental lithosphere beneath Somerset Island represent isotopically distinct domains and do not share a common petrogenetic history. The Lu–Hf isotope systematics of the shallow low-temperature peridotites define a positively sloped line that plot along a 2.8 Ga reference isochron. A number of these peridotites are characterized by highly radiogenic Hf isotopic compositions suggestive of long-term radiogenic ingrowth (billions of years). These findings are consistent with an interpretation that the shallow Somerset lithosphere (to depths of $\sim$150 km) stabilized in the Archean. The majority of the high-temperature peridotites plot closer to the composition of the host kimberlite. Although the observed isotopic variation may be attributed in part to kimberlite-related Hf addition, it is possible that these deep-seated xenoliths represent younger mantle. The superchondritic $^{176}Lu/^{177}Hf$ ratios observed for a number of the shallow low-temperature peridotites indicate strong fractionation of Lu and Hf, suggesting mantle root formation in the garnet stability field (depths >80 km). The Hf isotope compositions for the Somerset low-temperature peridotites indicate that part of the mantle root beneath the North American craton is characterized by a more radiogenic Hf isotope signature than that estimated for a typical 'depleted' mantle.

Keywords: Archean; lithosphere; Canadian; cratons; kimberlite; Lu–Hf; peridotites; mantle; xenoliths

* Corresponding author. Tel.: 1-514-987-3000, ext. 7019; Fax: 1-514-987-3635.
E-mail address: schmidberger.stefanie@courrier.uqam.ca (S.S. Schmidberger).

0012-821X/02/$ – see front matter
PII: S0012-821X(02)00491-0

1. Introduction

The mantle roots underlying the Archean cratons extend to depths of at least 200 km [1,2], and are depleted in basaltic constituents relative to fertile mantle (e.g. [3–5]). The lower density and higher viscosity of these refractory peridotite roots relative to the surrounding asthenosphere contribute to their stability and long-term isolation from the convecting mantle [6,7]. The isotopic diversity recorded by both continental peridotites and basalts compared to oceanic volcanics, along with their unusually 'enriched' Sr and Nd isotope signatures relative to bulk Earth ([8–10] and references therein) were the first indications of the antiquity of the subcratonic lithosphere [11,12]. These enriched isotope signatures are predominantly the result of repeated episodes of metasomatic activity, which have occurred since lithosphere stabilization (i.e. over billions of years [13,14]). Consequently, determining the age of Archean cratonic mantle roots has proven difficult. Re–Os isotope systematics appear to be less susceptible to metasomatic alteration, and have provided valuable age constraints for the subcontinental lithosphere [12]. Re depletion ages range from the mid to late Archean (3.5–2.7 Ga) for the mantle roots beneath South Africa, Siberia and North America [15–18]. In contrast to the abundant Nd, Pb, Sr and Os isotope data, the Hf isotope composition of subcontinental lithospheric mantle has yet to be investigated. This region constitutes an important reservoir in the Hf budget of the Earth's mantle, and establishing its Hf isotopic composition is important in order to better understand its origin, geochemical evolution, and its role in the stabilization of the Archean cratons.

The Lu–Hf isotopic system is characterized by the long-lived radioactive parent isotope ^{176}Lu that decays to ^{176}Hf by β emission with a half-life of 37 Ga [19,20], allowing the dating of ancient samples [21]. Lu (a heavy rare earth element, HREE) and Hf (a high field strength element) are both refractory silicate-hosted (e.g. [22]) elements, but exhibit significant differences in their geochemical behavior (e.g. different mineral/melt partition coefficients [23,24]) in the presence of mineral phases such as garnet and zircon. This can result in the strong fractionation of parent and daughter elements during magmatic and metamorphic processes, indicating the important potential of the Lu–Hf isotopic system in geochronology and as a geological tracer (e.g. [25–28]).

In this paper we report Hf isotopic compositions and ^{176}Lu/^{177}Hf ratios obtained using the MC-ICP-MS (multicollector inductively coupled plasma mass spectrometry) method for a suite of refractory peridotites and their constituent garnets from the Cretaceous (100 Ma) Nikos kimberlite on Somerset Island in the Canadian Arctic (Fig. 1) [29]. To our knowledge, these are the first Lu–Hf isotope data obtained for kimberlite-hosted mantle xenoliths to date. The main objective of this study is to constrain the Hf isotopic composition of the lithospheric mantle beneath the northern Canadian craton in order to contribute to a better understanding of the Hf isotope composition and evolution of the Earth's mantle. The data permit an evaluation of the effectiveness of the Lu–Hf geochronometer in providing meaningful age constraints on the stabilization of the mantle root. The results also provide information on elemental fractionation during partial melting at the time of lithosphere formation, and on the Hf isotopic composition of the Archean mantle.

2. Samples

2.1. Kimberlite

The Nikos kimberlite is part of the Somerset Island kimberlite field [30] that was emplaced ~100 Myr ago (U–Pb ages on perovskite [31,32]) into Archean crystalline basement (Nd model ages up to 3.0 Ga [33]) at the northern margin of the Canadian craton (Fig. 1). The Nikos host kimberlite occurs as three closely associated individual pipes (each ~50 m diameter and 30–40 m apart) that contain abundant mantle xenoliths. Unlike many other Somerset Island kimberlites, the southern Nikos pipe (NK3) exhibits a non-brecciated, magmatic texture [29]. Four kimberlite samples were collected from this magmatic pipe for analysis, two of which (NK3-K1, NK3-

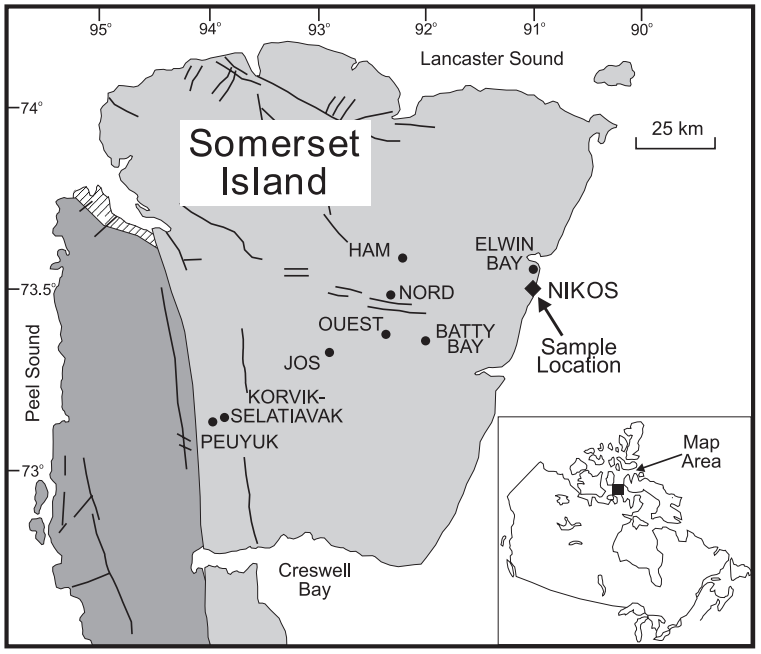

Fig. 1. Geological map of Somerset Island (after [52]) showing kimberlite locations. The mantle xenoliths from this study were collected from the Nikos kimberlite (black diamond). Legend: light gray, Paleozoic cover rocks; striped, Late Proterozoic cover rocks; dark gray, Precambrian basement; bold lines, normal faults.

K2) exhibit abundant mantle xenoliths relative to the remaining samples (NK3-K3, NK3-K4). The kimberlite contains olivine, phlogopite, garnet and spinel in a fine-grained matrix of calcite, serpentine, perovskite and apatite. Calcites occur as tabular euhedral crystals that are deflected around large olivine phenocrysts indicating their primary magmatic nature [29]. Two samples (NK3-K1, NK3-K2) are observed to contain garnet fragments in thin section, which probably represent xenocrysts. The Nikos kimberlite is characterized by very high whole-rock $CaCO_3$ contents (27–39 wt%), and a strong enrichment in incompatible trace elements such as LILE (large ion lithophile elements) and LREE (light rare earth elements) relative to chondrites and primitive mantle compositions [34,35].

2.2. Mantle xenoliths

The Nikos mantle xenoliths are large, well-preserved garnet peridotite nodules containing olivine, orthopyroxene, clinopyroxene, garnet and minor phlogopite ($\sim$1 wt% or less [29]). One spinel peridotite (NK2-9) consists of olivine, orthopyroxene, clinopyroxene and chromian spinel. The majority of the xenoliths exhibit coarse textures, and only minor occurrences of porphyroclastic textures are observed (e.g. NK1-7). The peridotites are characterized by refractory major element chemistry and have high Mg# (Mg# = Mg/[Mg+Fe] = 0.90–0.93) suggesting that they are melt-depleted residues. Despite their depleted major element compositions, the Nikos peridotites are enriched in highly incompatible trace elements (e.g. LILE, LREE), while having approximately chondritic HREE contents. Mass balance calculations indicate that constituent peridotite minerals control HREE budgets, but cannot account for the high LREE abundances observed in the whole rocks, suggesting the presence of small amounts of a kimberlite-related LREE-rich interstitial component (i.e. $\sim$1% kimberlite liquid) and/or accessory mineral (i.e. trace amounts of apatite [35]).

The Nikos peridotites and constituent minerals

have Sr and Pb isotopic signatures and incompatible trace element compositions (e.g. La/Sm_N) that correlate with temperature and pressure (and thus depth) estimates of last equilibration, suggesting that the samples can be divided into low-temperature (800–1100°C; 25–50 kb; 80–150 km) and high-temperature peridotites (1100–1400°C; 50–60 kb; 150–180 km) [35,36]. The low-temperature peridotites and clinopyroxenes are characterized by less radiogenic $^{87}Sr/^{86}Sr_{(0.1Ga)}$ (0.7038–0.7066) and higher $^{206}Pb/^{204}Pb_{(0.1Ga)}$ (17.82–19.03) signatures at the time of kimberlite emplacement than those of the high-temperature peridotites ($^{87}Sr/^{86}Sr_{(0.1Ga)} = 0.7052–0.7095$; $^{206}Pb/^{204}Pb_{(0.1Ga)} = 17.18–18.30$). In addition, the low-temperature xenoliths show a stronger enrichment in incompatible trace elements (average $La/Sm_N = 6$) relative to those in the high-temperature xenoliths (average $La/Sm_N = 3$). These results indicate that the shallow low-temperature and the deep high-temperature lithosphere represent chemically distinct mantle reservoirs that do not share a common petrogenetic history [36]. In comparison, Nd isotopic compositions of low- and high-temperature peridotites ($^{143}Nd/^{144}Nd_{(0.1Ga)} = 0.51255–0.51276$ and 0.51242–0.51262, respectively), which are slightly depleted compared to CHUR (chondrite uniform reservoir), overlap, and they are similar to those of the Nikos kimberlite ($^{143}Nd/^{144}Nd_{(0.1Ga)} = 0.51254–0.51259$). More detailed discussions on mineralogy, and geochemical and isotopic composition of the peridotites and their host kimberlite can be found in [29,35,36].

2.3. Garnets

The Nikos garnets are chromian pyropes and their major element chemistry indicates that the crystals are compositionally homogeneous on a thin section scale [29]. The garnets in the low-temperature peridotites are characterized by low Mg# (0.81–0.84), low TiO_2 (0.08–0.09 wt%) and Zr (10–50 ppm) contents, and high FeO (7.2–7.9 wt%) and MnO (0.4–0.5 wt%) abundances compared to those in the high-temperature peridotites (Mg# = 0.83–0.86; TiO_2 = 0.1–0.3 wt%; Zr = 35–100 ppm; FeO = 6.2–7.2 wt%; MnO = 0.3–0.4 wt% [35]). Sr isotopic compositions for garnets in the high-temperature peridotites ($^{87}Sr/^{86}Sr_{(0.1Ga)} = 0.7067–0.7095$) extend to more radiogenic values than those for garnets in the low-temperature peridotites ($^{87}Sr/^{86}Sr_{(0.1Ga)} = 0.7061–0.7073$) at the time of kimberlite emplacement [36].

3. Analytical methods

All exterior surfaces were first removed from the peridotites. The xenoliths were then crushed and rock chips were ground in an aluminum mill. Garnet separates were handpicked under a binocular microscope and inclusion-free grains were washed in an ultrasonic bath with acetone, ultrapure water and 2.5 N HCl, and then ground to small fragments in an agate mill. Crushed kimberlite whole rocks were carefully handpicked under a binocular microscope prior to grinding in an attempt to eliminate contamination from peridotite xenocrysts and country rock fragments.

For Lu–Hf isotope analysis, the sample powders (~0.8–1 g for whole rocks and ~0.2–0.25 g for garnets) were spiked with separate ^{180}Hf (98.3% enriched) and ^{176}Lu (70.9% enriched) tracers prior to dissolution. The ^{180}Hf contribution from the Hf isotope tracer represented ~3% of the total ^{180}Hf in the mixtures in order to minimize the correction of the measured $^{176}Hf/^{177}Hf$ ratio for spike addition [21]. Whole-rock samples and garnet separates were dissolved in a mixture of $HF–HNO_3–HClO_4$ in Teflon bombs at 170°C for at least 10 days in order to ensure complete digestion and sample–spike homogenization. Prior to analysis, Hf was isolated from the REE in a fluoride precipitation step and then purified using a two-stage elution procedure (anion and cation exchange [21]). Lu was separated as part of the REE fraction on a cation exchange column [21], then isolated from the LREE fraction using HDEHP columns. Total procedural blanks for Hf and Lu were less than 20 pg, a factor of at least 1000 for Hf and 800 for Lu lower than the total amount of Hf and Lu processed in the least abundant samples, thus rendering the blank correction negligible.

Hf and Lu isotope measurements were obtained using a Micromass IsoProbe MC-ICP-MS at GEOTOP, Université du Québec à Montréal. The Hf isotopic data were acquired in static, multicollection mode using eight Faraday collectors with cup efficiencies set at unity. The mass configuration array included monitoring of isobaric interferences using isotopes ^{182}W (for ^{180}W), ^{175}Lu (for ^{176}Lu) and ^{173}Yb (for ^{176}Yb), identical to that outlined in [37]. ^{181}Ta was not monitored for potential interferences of ^{180}Ta on ^{180}Hf because of the extremely low abundances of Ta ($\ll$0.1 ppm) in the peridotite samples [35], combined with the very low natural abundance ($\sim$0.012%) of ^{180}Ta. At the start of each analytical session, a 50 ppb solution of the JMC 475 Hf standard was aspirated into the ICP source using an ARIDUS® microconcentric nebulizer at an uptake rate of $\sim$50 μl/min and analyzed for approximately 10 min. This corresponds to $\sim$25 ng of total Hf consumed per analysis, roughly the same magnitude as that processed for the samples used in this study. The uptake rate of the ARIDUS® instrument was kept constant and verified on a regular basis; sweep gas settings were optimized to yield maximum ion signal intensity and minimize oxide levels. The level of Hf oxide was typically $\leq$0.1% of the ion signal for the metal. The intensity of the ion signal was typically 2.0×10^{-11} A of ^{180}Hf corresponding to an absolute sensitivity of $\sim$120 V/ppm. Data acquisition consisted of a 50 s 'on-peak-zero' baseline measurement (i.e. gas and 2% HNO_3 blank) with the same 2% HNO_3 solution used to dilute the samples. Subsequent to sample introduction, two half-mass unit baseline measurements were obtained within the mass range 172.5–182.5, bracketing the mass range used for data acquisition. The JMC 475 standard and samples were analyzed for one block of 50 scans with a 10 s integration time per cycle. The measured Hf isotopic ratios were normalized to $^{179}Hf/^{177}Hf = 0.7325$ and corrected for mass bias using the exponential law [38]. Removal of 'spike addition' was achieved using an iterative calculation [21]. Repeated measurements ($n = 22$) of the JMC 475 standard (in 2% HNO_3) during the course of this study (April 2000 to May 2001) yielded the following results: $^{176}Hf/^{177}Hf = 0.282158 \pm 23$, $^{178}Hf/^{177}Hf = 1.46727 \pm 13$ and $^{180}Hf/^{177}Hf = 1.88669 \pm 21$ (2σ standard deviation errors). Solutions made from high-purity Lu and Yb metals from the Ames laboratory (20 and 10 ppb, respectively) and W (100 ppb) were analyzed prior to the measurement of samples in order to determine their mass bias and thus accurately correct for isobaric interferences, if present. However, intensities of ^{175}Lu, ^{173}Yb and ^{182}W were at or below the limit of detection for the majority of the samples. For spiked ^{176}Lu isotope dilution analyses, Yb is not separated from Lu in the chemical procedure. Thus careful evaluation of their respective mass biases is warranted in order to correct for the isobaric interference of ^{176}Yb on ^{176}Lu. Prior to sample analysis, the mass biases for Lu and Yb were determined by measuring the $^{176}Lu/^{175}Lu$ and $^{176}Yb/^{173}Yb$ for solutions of Ames Lu (20 ppb) and Yb (10 ppb) metals, and then compared to the recommended values of 0.02656 and 0.78761 [21], respectively. Evaluation of this correction was determined using a series ($n = 8$) of Yb-doped and ^{176}Lu-spiked gravimetrically prepared Ames Lu solutions. The quantity of Lu used in these solutions matched that for the peridotites; however, their Yb/Lu values were double those of the samples so as to purposely exaggerate the correction. The results indicate that the calculated Lu concentrations reproduce to better than 0.2% (2σ level). Moreover, the reproducibility for calculation of the isotopic compositions and concentrations of Hf was evaluated by a triplicate analysis (on three separate dissolutions of the same powder) of a fine-grained calc-alkaline basalt, which yielded $^{176}Hf/^{177}Hf$ values of 0.282633 ± 11, 0.282638 ± 8, 0.282636 ± 8 and Hf concentrations of 3.47, 3.46, 3.48 ppm, respectively. The latter are identical to a Hf concentration of 3.42 ± 0.17 ppm obtained by conventional ICP-MS analysis [39], despite the fact that the abundance of Ta (0.4 ppm [39]) in the basalt is more than four times the concentration of Ta measured in the Nikos peridotites.

4. Results

4.1. Kimberlite

The two kimberlite samples containing the lowest amounts of peridotite xenoliths (NK3-K3, NK3-K4) are characterized by low $^{176}Lu/^{177}Hf$ ratios (0.003) and have chondritic to slightly superchondritic [40] initial $^{176}Hf/^{177}Hf_{(0.1Ga)}$ (0.282711 and 0.282852), corresponding to initial $\varepsilon_{Hf(0.1Ga)}$ values of 0 and +5.0 (Table 1; Fig. 2a). Two kimberlite samples (NK3-K1, NK3-K2) that contained abundant mantle xenoliths also have low $^{176}Lu/^{177}Hf$ ratios (0.004), but higher initial $^{176}Hf/^{177}Hf_{(0.1Ga)}$ (0.283191 and 0.283307; initial $\varepsilon_{Hf(0.1Ga)} = +17$ and +21.1). Kimberlites from South Africa have been divided into two groups ('Group I' and 'Group II') based on their distinct mineralogy and Sr–Nd–Pb isotopic signatures (e.g. [41,42]). Recent studies have shown that both South African 'Group I' and 'Group II' kimberlites are characterized by low $^{176}Lu/^{177}Hf$ ratios similar to those of the Nikos kimberlite (Fig. 2a) [43]. The initial $\varepsilon_{Hf(0.1Ga)}$ values for two Nikos

Table 1
Lu–Hf isotope data for Nikos peridotites and kimberlite

Sample	Temperature (°C)	Pressure (kb)	Lu (ppm)	Hf (ppm)	$^{176}Lu/^{177}Hf$	$^{176}Hf/^{177}Hf$ (measured)	$^{176}Hf/^{177}Hf_{(0.1Ga)}$	ε_{Hf}	$\varepsilon_{Hf(0.1Ga)}$
Low-temperature peridotites									
NK1-4	871	33.5	0.0227	0.0768	0.0422	0.283900 ± 20	0.283821	39.9	39.3
NK1-4 Dup.			0.0289	0.0923	0.0446	0.284072 ± 20	0.283988	46.0	45.2
NK2-3	887	34.6	0.0371	0.1389	0.0381	0.283566 ± 23	0.283495	28.1	27.8
NK1-23	964	39.0	0.0349	0.1722	0.0289	0.283344 ± 30	0.283290	20.2	20.5
NK1-23 Dup.				0.1905		0.283342 ± 28		20.2	
NK1-14	1027	42.7	0.0198	0.0589	0.0480	0.284280 ± 28	0.284190	53.3	52.3
NK1-14 Dup.			0.0209	0.0658	0.0452	0.284152 ± 26	0.284068	48.8	48.0
NK1-2	1042	44.7	0.0160	0.0720	0.0316	0.283662 ± 33	0.283603	31.5	31.6
NK1-2 Dup.			0.0167	0.0694	0.0343	0.283885 ± 19	0.283820	39.3	39.3
NK1-3	1076	46.5	0.0182	0.0966	0.0269	0.283014 ± 14	0.282963	8.5	9.0
NK1-3 Dup.				0.0905		0.282989 ± 14		7.7	
NK2-9[a]	808		0.0028	0.0142	0.0284	0.283180 ± 58	0.283127	14.4	14.7
High-temperature peridotites									
NK1-6	1149	48.8	0.0080	0.0718	0.0159	0.283164 ± 16	0.283134	13.9	15.0
NK2-1	1216	51.5	0.0074	0.1080	0.0097	0.282884 ± 30	0.282866	4.0	5.5
NK1-9	1219	53.4	0.0173	0.1624	0.0152	0.282834 ± 07	0.282805	2.2	3.4
NK1-19	1228	51.9	0.0064	0.0588	0.0155	0.283012 ± 13	0.282983	8.5	9.7
NK1-19 Dup.			0.0058	0.0589	0.0141	0.283139 ± 15	0.283113	13.0	14.3
NK3-25	1256	54.0	0.0281	0.3038	0.0132	0.282679 ± 51	0.282654	−3.3	−2.0
NK1-5	1262	54.6	0.0177	0.2091	0.0121	0.282805 ± 14	0.282782	1.2	2.6
NK1-7[b]	1300	55.1	0.0164	0.0669	0.0349	0.283364 ± 15	0.283298	20.9	20.8
NK1-7 Dup.			0.0187	0.0798	0.0334	0.283389 ± 16	0.283326	21.8	21.8
NK2-2	1316	54.7	0.0220	0.1637	0.0191	0.283248 ± 24	0.283212	16.8	17.8
NK1-10	1405	63.7	0.0043	0.1682	0.0037	0.282874 ± 20	0.282867	3.6	5.6
Kimberlite									
NK3-K1			0.0751	2.973	0.0036	0.283197 ± 25	0.283191	15.0	17.0
NK3-K2			0.0730	2.648	0.0039	0.283314 ± 39	0.283307	19.2	21.1
NK3-K3			0.0899	3.751	0.0034	0.282858 ± 13	0.282852	3.1	5.0
NK3-K4			0.0574	2.821	0.0029	0.282716 ± 37	0.282711	−2.0	0

[a] Spinel peridotite.

[b] Porphyroclastic texture. $\varepsilon_{Hf(0.1Ga)}$ values calculated for 100 Ma in situ decay using present-day ratios of $^{176}Hf/^{177}Hf_{(CHUR)} = 0.282772$ and $^{176}Lu/^{177}Hf_{(CHUR)} = 0.0332$ [40] and $\lambda = 1.876 \times 10^{-11}$ yr^{-1} [19,20]. Precision for individual Hf isotope measurements is quoted at the 2σ level. Lu and Hf concentrations were determined by isotope dilution analysis; uncertainties for $^{176}Lu/^{177}Hf$ are ∼2%.

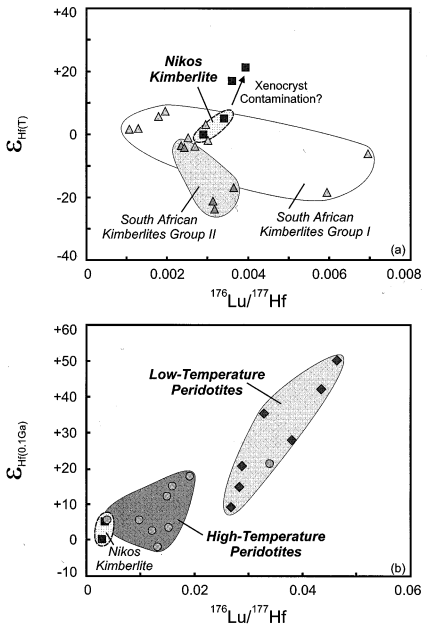

Fig. 2. (a) $^{176}Lu/^{177}Hf$ versus initial $\varepsilon_{Hf(T)}$ (100 Ma) for the Nikos kimberlite. Also shown are two samples that most likely experienced contamination by xenocrystic garnet (for further explanation see text). Data for South African 'Group I' (90–110 Ma) and 'Group II' (120–150 Ma) kimberlites are shown for comparison [43]. (b) $^{176}Lu/^{177}Hf$ versus $\varepsilon_{Hf(0.1Ga)}$ for Nikos peridotites at the time of kimberlite emplacement. For samples with duplicate analyses, the average composition is plotted.

kimberlite samples plot within the field of initial $\varepsilon_{Hf(T)}$ values for South African 'Group I' kimberlites, while those samples that contained abundant peridotite plot towards higher values. South African 'Group II' kimberlites, in comparison, are characterized by negative initial $\varepsilon_{Hf(T)}$ values (Fig. 2a).

4.2. Mantle xenoliths

The low-temperature peridotites exhibit a significant range of $^{176}Lu/^{177}Hf$ ratios (0.027–0.048) and have radiogenic Hf isotopic compositions ($^{176}Hf/^{177}Hf_{(0.1Ga)}$ = 0.282963–0.284190; $\varepsilon_{Hf(0.1Ga)}$ = +9.0 to +52.3) at the time of kimberlite emplacement (Table 1; Fig. 2b). In comparison, the high-temperature peridotites are characterized by lower $^{176}Lu/^{177}Hf$ ratios (0.004–0.016) and, in general, less radiogenic Hf isotopic compositions ($^{176}Hf/^{177}Hf_{(0.1Ga)}$ = 0.282654–0.283212; $\varepsilon_{Hf(0.1Ga)}$ = −2.0 to +17.8; Fig. 2b). The Hf isotopic compositions of all Nikos peridotites (except one sample, NK3-25) are depleted relative to a chondritic reservoir [40]. One high-temperature xenolith (NK1-7), which in contrast to most other samples is characterized by a porphyroclastic texture, has $^{176}Lu/^{177}Hf$ and $^{176}Hf/^{177}Hf_{(0.1Ga)}$ ratios (0.035 and 0.283312, respectively; $\varepsilon_{Hf(0.1Ga)}$ = +21.3; average of duplicate analyses; Fig. 2b) similar to those of the low-temperature peridotites.

In a $^{176}Lu/^{177}Hf$ versus $^{176}Hf/^{177}Hf$ diagram, the data for the low-temperature xenoliths show a positively sloped correlation. The regression line for the Lu–Hf data indicates that this array corresponds to an errorchron age of 2.8 ± 0.8 Ga (n = 6; MSWD = 24) with an initial $^{176}Hf/^{177}Hf$ ratio of 0.28164 ± 57 (ε_{Hf} = +23; Fig. 3). One low-temperature sample (NK1-2) is not included in the data regression as the presence of carbonate-rich veins suggests kimberlite contamination (open symbol; Fig. 3). Since the low-temperature peridotites were sampled over a large depth interval (80–150 km) and the errorchron age is associated with a large error, a 2.8 Ga reference isochron with a corresponding initial Hf isotopic ratio is plotted for comparison rather than the errorchron (Fig. 3). The majority of the high-temperature peridotites exhibit lower $^{176}Lu/^{177}Hf$ ratios and trend towards the composition of the Nikos kimberlite (Table 1; Fig. 2b). No data plot to the right of the reference isochron.

Duplicate analyses were obtained on separate dissolutions of the rock powders (not on sample splits after initial dissolution). The $^{176}Lu/^{177}Hf$ ratios vary by 5–8% and Hf isotope ratios by 4–8 ε_{Hf} units for the low-temperature peridotites (NK1-4, NK1-14, NK1-2; Table 1). Although these variations are relatively large, in each case the parent–daughter ratio correlates with isotopic composition. The variations in the Lu/Hf ratios and Hf isotopic compositions are thus attributed to sample heterogeneity of the whole-rock powders, resulting from the coarse-grained nature of the peridotites, in particular, the presence of large crystals of garnet (up to 5 mm), and their (Archean) age. Duplicate analyses of Hf isotopic composition for two other low-temperature peridotites

(NK1-23, NK1-3) are within error. For two high-temperature peridotites (NK1-19, NK1-7) parent–daughter ratios do not correlate with isotopic ratios, which is probably the result of kimberlite contamination (see later discussion). For samples with duplicate $^{176}Lu/^{177}Hf$ and Hf isotope ratios, these are plotted as average values in the figures.

4.3. Garnets

The garnets of the low-temperature xenoliths exhibit a large range of $^{176}Lu/^{177}Hf$ ratios (0.093–0.243) and their $^{176}Hf/^{177}Hf_{(0.1Ga)}$ compositions (0.283096–0.286947; $\varepsilon_{Hf(0.1Ga)} = +13.7$ to +150) extend to extremely radiogenic values at the time of kimberlite emplacement (Table 2). In comparison, the garnets from the high-temperature peridotites have lower $^{176}Lu/^{177}Hf$ ratios (0.015–0.057) and less radiogenic $^{176}Hf/^{177}Hf_{(0.1Ga)}$ compositions (0.282749–0.283407; $\varepsilon_{Hf(0.1Ga)} = +1.4$ to +24.7; Table 2). The garnets from the low-temperature peridotites are characterized by slightly higher Lu (average 0.30 ppm), but significantly lower Hf abundances (average 0.31 ppm) than garnets from the high-temperature peridotites (average Lu = 0.25 ppm; Hf = 0.95 ppm; Table 2). Tie lines for individual garnet–whole-rock pairs in the low-temperature peridotites are all positively sloped and correspond to internal isochrons 'ages' ranging from 900 to 250 Ma (Table 2; Fig. 4). In contrast, the garnet–whole-rock tie lines for most high-temperature peridotites (except porphyroclastic xenolith NK1-7; 330 Ma) define negative (or flat) trends (Fig. 4). Duplicate analyses of garnet separate NK1-7 yield a difference of ~0.9% for the $^{176}Lu/^{177}Hf$ value and identical $^{176}Hf/^{177}Hf$ compositions (Table 2), supporting our interpretation that sample heterogeneity is responsible for the variation exhibited by the replicate analyses of the whole-rock powders.

5. Discussion

5.1. Kimberlite mantle source

Two Nikos kimberlite samples (NK3-K3, NK3-K4) are characterized by chondritic or slightly superchondritic initial Hf isotope compositions ($\varepsilon_{Hf(0.1Ga)} = 0$ and +5.0), and these plot within the field of Lu–Hf isotope data for South African kimberlites (Fig. 2a) [43]. In comparison, initial $\varepsilon_{Hf(0.1Ga)}$ values (+17 and +21.1; NK3-K1,

Table 2
Lu–Hf isotope data for Nikos garnets

Sample	Temperature (°C)	Pressure (kb)	Lu (ppm)	Hf (ppm)	$^{176}Lu/^{177}Hf$	$^{176}Hf/^{177}Hf$ (measured)	$^{176}Hf/^{177}Hf_{(0.1Ga)}$	ε_{Hf}	$\varepsilon_{Hf(0.1Ga)}$	Date (Ma)
Low-temperature garnets										
NK1-4 Gt	871	33.5	0.2742	0.1609	0.2430	0.287403 ± 59	0.286947	164	150	905
NK2-3 Gt	887	34.6	0.2812	0.2262	0.1774	0.285589 ± 15	0.285256	99.6	90.1	769
NK2-10 Gt	1014	42.1	0.2636	0.4060	0.0926	0.283270 ± 37	0.283096	17.6	13.7	499
NK1-14 Gt	1027	42.7	0.2741	0.2238	0.1747	0.285419 ± 13	0.285091	93.6	84.2	
NK1-2 Gt	1042	44.7	0.3667	0.3479	0.1503	0.284465 ± 18	0.284183	59.9	52.1	313
NK1-3 Gt	1076	46.5	0.3255	0.4952	0.0937	0.283309 ± 11	0.283133	19.0	15.0	235
High-temperature garnets										
NK2-1 Gt	1216	51.5	0.1670	1.549	0.0154	0.282778 ± 08	0.282749	0.2	1.4	
NK1-9 Gt	1219	53.4	0.2516	1.064	0.0337	0.282831 ± 09	0.282768	2.1	2.1	
NK1-5 Gt	1262	54.6	0.2148	1.229	0.0249	0.282873 ± 07	0.282826	3.6	4.1	
NK3-16 Gt	1280	53.5	0.3539	1.024	0.0493	0.282993 ± 15	0.282900	7.8	6.7	
NK1-7 Gt	1300	55.1	0.2442	0.6252	0.0557	0.283512 ± 13	0.283407	26.2	24.7	326
NK1-7 Gt Dup.			0.2411	0.6117	0.0562	0.283509 ± 71	0.283403	26.1	24.5	
NK2-2 Gt	1316	54.7	0.2666	0.8145	0.0467	0.283165 ± 74	0.283078	13.9	13.0	
NK3-4 Gt	1371	58.5	0.2702	0.6780	0.0568	0.283508 ± 22	0.283401	26.0	24.5	

Analytical procedures as in Table 1. Date refers to internal isochron 'age' using garnet–whole-rock pairs.

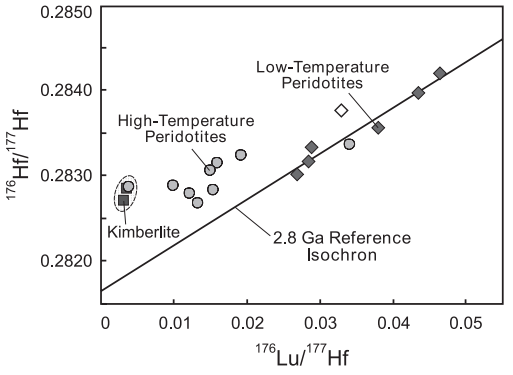

Fig. 3. $^{176}Lu/^{177}Hf$ versus $^{176}Hf/^{177}Hf$ diagram for Nikos peridotites. 2.8 Ga Lu–Hf reference isochron is plotted, which corresponds to the regression line for data (and corresponding initial $^{176}Hf/^{177}Hf$) for the low-temperature peridotites (solid diamonds). See text for further details.

NK3-K2) for two kimberlite samples that contain abundant mantle xenoliths are much higher. The significant variation in Hf isotope ratios could be inherited from a (non-homogeneous) kimberlite mantle source, or indicate the presence of xenocrysts (e.g. garnet) in the kimberlite derived by fragmentation of peridotite xenoliths. It appears likely that xenocrystic garnet (as observed in thin sections) is responsible for the high $\varepsilon_{Hf(0.1Ga)}$ values of two kimberlite samples (NK3-K1, NK3-K2), since it has high $^{176}Lu/^{177}Hf$ and thus high time-integrated Hf isotopic ratios. This interpretation is supported by $\varepsilon_{Nd(0.1Ga)}$ values (+1.1 and +0.6, respectively) [36] that correlate negatively with $\varepsilon_{Hf(0.1Ga)}$ values in these two samples, the opposite of what is observed for most terrestrial rocks [44].

The kimberlite samples that are characterized by low $\varepsilon_{Hf(0.1Ga)}$ values (NK3-K3, NK3-K4) are interpreted to represent the Hf isotopic composition of the Nikos kimberlite at the time of emplacement, and these are plotted in the figures. Since kimberlites represent low degree partial melts (1% or less [45]), the small difference in their $\varepsilon_{Hf(0.1Ga)}$ values (0 and +5.0) may be attributed to the inhomogeneous composition of the mantle source. In a Hf–Nd diagram, the two Nikos kimberlite samples exhibit a positive correlation of these isotope ratios with chondritic to slightly superchondritic compositions, and plot within the terrestrial Hf–Nd array (Fig. 5).

5.2. Shallow versus deep lithosphere

The refractory major element compositions of the Nikos peridotites that sample the Somerset lithosphere indicate that these xenoliths are melt-depleted residues [29]. The Lu abundances of both the low- and high-temperature peridotites show a good positive correlation with their bulk rock Al_2O_3 contents, which constitute a measure for the degree of major element depletion in residual peridotites (Fig. 6). These findings suggest that the Lu levels observed in these xenoliths were controlled by variable degrees of partial melting during lithosphere formation.

The low-temperature Nikos peridotites were sampled over a very large depth interval of about 70 km by their host kimberlite. These xenoliths are characterized by Lu–Hf isotopic compositions that plot close to a line corresponding to a reference isochron age of 2.8 Ga (Fig. 3). This reference isochron age is almost identical to Re depletion ages (2.7 Ga) that were recently reported for other Somerset Island peridotites [18]. A number of the low-temperature peridotites exhibit very radiogenic Hf isotopic compositions at the time of kimberlite magmatism ($^{176}Hf/^{177}Hf_{(0.1Ga)}$ =0.2835–0.2841, $\varepsilon_{Hf(0.1Ga)}$ = +30 to +50; Table 1; Figs. 2b, 5) compared to estimates for a typical 'depleted' mantle (~0.2832, +18, respectively [40, 46]. Long-term (billions of years) radiogenic in-

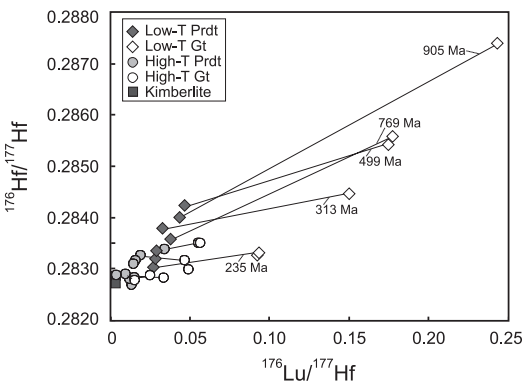

Fig. 4. $^{176}Lu/^{177}Hf$ versus $^{176}Hf/^{177}Hf$ diagram for Nikos garnets and peridotites. Tie lines connect garnet with corresponding whole-rock composition. Also shown are the 'dates' (in million years) obtained for individual internal Lu–Hf isochrons using garnet–whole-rock pairs.

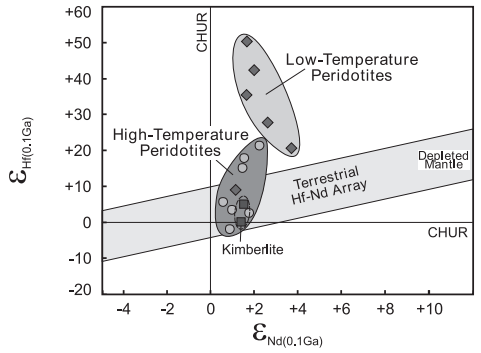

Fig. 5. Hf–Nd variation diagram for Nikos peridotites at the time of kimberlite emplacement (Nd data from [36]). The Hf–Nd array for terrestrial samples [44] and the composition of 'depleted' mantle are plotted for comparison [8,40,46].

growth is required to produce the highly depleted Hf isotopic signatures. These results provide evidence for an ancient (Archean) depletion event that resulted in the stabilization of the mantle root beneath the northern Canadian craton to depths of about 150 km. The initial Hf isotopic value ($^{176}Hf/^{177}Hf = 0.28164 \pm 57$) associated with this reference isochron corresponds to an ε_{Hf} value of +23 but with the error could be as low as +3. These results suggest that the low-temperature Nikos peridotites were derived from a mantle having melt-depleted characteristics at the time of lithosphere stabilization rather than from a primitive mantle reservoir [40,46]. A number of the low-temperature Nikos xenoliths are characterized by slightly subchondritic $^{176}Lu/^{177}Hf$ ratios (< 0.033), while having superchondritic Hf isotopic compositions ($^{176}Hf/^{177}Hf > 0.282772$ [40]), suggesting recent perturbation of their $^{176}Lu/^{177}Hf$ ratios. Since Lu levels correlate with other indices of melt depletion and thus appear to have been controlled by partial melting (Fig. 6), these xenoliths may have experienced minor Hf addition rather than Lu loss. The Nikos kimberlite is characterized by low $^{176}Lu/^{177}Hf$ ratios and high Hf abundances, and it appears likely that these xenoliths may have been affected by interaction with the host magma during sample transport. The addition of very small amounts of a kimberlite component ($\sim 0.5\%$ bulk kimberlite or significantly less of a kimberlite-related Hf-bearing accessory mineral) as indicated by mass balance calculations, would produce slightly subchondritic $^{176}Lu/^{177}Hf$ ratios. In contrast to the low-temperature xenoliths, the majority of the high-temperature peridotites plot closer to the composition of the kimberlite (Figs. 2b, 3). This feature could be interpreted as the result of more extensive contamination with host kimberlite since these xenoliths resided closer to the area of kimberlite formation, and/or that these peridotites are younger and represent mantle of distinct origin.

The highly variable Hf isotopic compositions of the Nikos peridotites are predominantly superchondritic at the time of kimberlite magmatism (Fig. 5). A number of the peridotites extend to significantly higher Hf values compared to 'depleted' mantle and plot above the terrestrial Hf–Nd array [44]. In comparison, the Nd isotopic compositions of the peridotites ($\varepsilon_{Nd(0.1Ga)} = +1$ to +4 [36]), which are distinctly lower than estimates for 'depleted' mantle ($\varepsilon_{Nd(0.1Ga)} \approx +10$; Fig. 5 [8]), show little variation, and overlap those of the Nikos kimberlite ($\varepsilon_{Nd(0.1Ga)} = +1$ to +2; Fig. 5). The Nd isotope results have been interpreted to indicate that the xenoliths were contaminated with small amounts of host magma during sample transport [36]. In contrast to tightly constrained Nd isotopic signatures, the low-temperature peridotites are characterized by significantly less radiogenic Sr (Fig. 7) and higher Pb (not shown) isotopic compositions ($^{87}Sr/^{86}Sr_{(0.1Ga)} = 0.7051$–$0.7066$; $^{206}Pb/^{204}Pb_{(0.1Ga)} = 17.82$–$19.03$) than the high-temperature peridotites ($^{87}Sr/^{86}Sr_{(0.1Ga)} =$

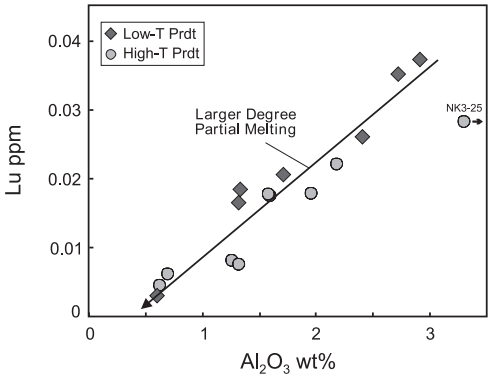

Fig. 6. Lu (ppm) versus Al_2O_3 contents (wt%) for Nikos peridotites (Al_2O_3 data from [35]).

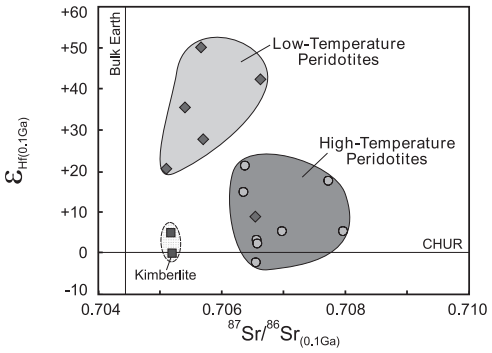

Fig. 7. $\varepsilon_{Hf(0.1Ga)}$ versus $^{87}Sr/^{86}Sr_{(0.1Ga)}$ for Nikos peridotites (Sr data from [36]).

0.7064–0.7080; $^{206}Pb/^{204}Pb_{(0.1Ga)}$ = 17.18–18.30). In addition, the Sr isotope ratios of the Nikos peridotites, with the exception of one sample (NK1-23), differ from those of the host kimberlite (Fig. 7 [36]). The distinct Sr and Pb isotope compositions of low- and high-temperature peridotites restrict the amount of interstitial kimberlite component to less than 1 wt% [36] as kimberlite contribution in excess of this amount would eradicate the observed isotopic differences. The Hf isotopic compositions of the Nikos peridotites are highly variable and the majority extend to significantly more radiogenic compositions than the host kimberlite (Figs. 2b, 5). As the average Hf abundance ratio (kimberlite/peridotite) of 20:1 is similar to that for Sr, but three times lower than for Nd (60:1), Hf is significantly less susceptible to kimberlite contamination than Nd. Since kimberlite addition was restricted to very small amounts, it is likely that the Hf isotopic differences observed for the Nikos peridotites existed prior to the kimberlite event (Figs. 2b, 5).

While all the Nikos xenoliths are refractory residues that were generated by extensive melt extraction, the low-temperature peridotites exhibit $\varepsilon_{Hf(0.1Ga)}$ values (+9 to +50) that are significantly higher and more variable than those of the high-temperature peridotites (−2 to +20). The distinct Hf isotopic compositions for low- and high-temperature peridotites are in agreement with the previously reported differences in Sr and Pb isotope compositions [36] indicating that shallow and deep Somerset lithosphere do not share a common petrogenetic history. The depth stratification could have resulted from infiltration of the lower lithosphere with metasomatic melts or fluids. This model cannot be reconciled, however, with the significantly less enriched incompatible trace element signatures of the deep-seated peridotites (average $La/Sm_N = 3$) relative to those of the shallow xenoliths (average $La/Sm_N = 6$ [35]). Alternatively, the deep lithosphere could be younger and was added to the Archean subcratonic mantle by downward growth of the shallow lithosphere, an interpretation consistent with the isotopic and trace element record [35,36]. Mantle stratification and post-Archean lithosphere growth have previously been proposed for other cratonic areas such as the Kaapvaal craton beneath South Africa (e.g. [10,16]) and appear to be a common feature for the lithospheric mantle root beneath the continents.

5.3. Garnet Hf isotope systematics

The garnets from the low-temperature peridotites are characterized by low Hf abundances (average 0.31 ppm) and their highly variable $^{176}Hf/^{177}Hf_{(0.1Ga)}$ compositions (0.28310–0.28695) extend to significantly more radiogenic values than those for garnets from the high-temperature peridotites (average Hf = 0.95 ppm; $^{176}Hf/^{177}Hf_{(0.1Ga)}$ = 0.28275–0.28341; Table 2; Fig. 4). These signatures correlate with chemical characteristics such as TiO_2 contents that are lower for garnets from the shallow peridotites (0.08–0.09 wt%) relative to those for garnets from the deep-seated peridotites (0.1–0.3 wt% [35]). The results indicate significant isotopic and chemical differences for garnets from low- and high-temperature Nikos peridotites, and are consistent with the finding based on the whole-rock Hf, Sr and Pb isotopic compositions that shallow and deep Somerset lithosphere represent mantle of distinct origin.

Internal Lu–Hf isochrons using garnet–whole-rock pairs (Fig. 4) for the low-temperature peridotites yield 'ages' ranging from 900 to 500 Ma, and 300 to 250 Ma for two samples that could have experienced minor kimberlite addition as suggested by the presence of carbonate-rich veins (NK1-2) and a slightly subchondritic $^{176}Lu/^{177}Hf$

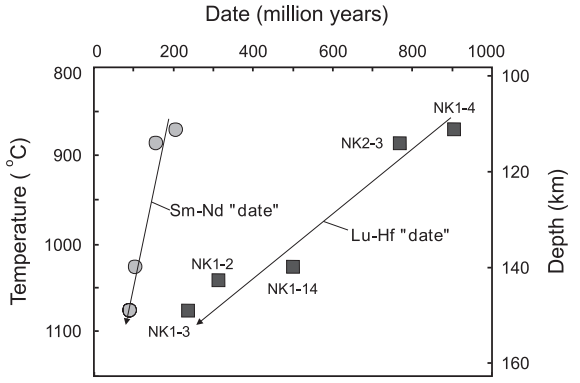

Fig. 8. Lu–Hf and Sm–Nd internal isochron 'dates' versus temperature (and depth) of last equilibration for low-temperature garnet–whole-rock pairs (Sm–Nd data from [36]).

ratio (NK1-3). The 'dates' defined by the Lu–Hf whole-rock–garnet isochrons decrease with increasing temperature (and thus depth), and the oldest 'age' is obtained for the shallowest garnet–whole-rock pair (870°C, 100 km; Fig. 8). No garnet–whole-rock pair at any depth, however, defines an internal isochron corresponding to an Archean age. These findings indicate that lithospheric temperatures (870°C and higher) exceeded the closure temperatures for Hf (and Lu) diffusion in the garnet–whole-rock system. The depth correlation of the Lu–Hf 'ages' suggests that the extent of Hf isotope re-equilibration in the garnet–whole-rock system varied as a function of temperature. In comparison, internal Sm–Nd isochrons for these same garnet–whole-rock pairs yield 'ages' of 200–90 Ma, and the youngest 'date' essentially coincides with the age of kimberlite formation [36]. The Lu–Hf 'date' for individual garnet–whole-rock pairs is always older than that obtained using Sm–Nd systematics. Although Nd isotope systematics appear to be more susceptible to kimberlite contamination, these findings are also consistent with recent results based on high-grade metamorphic rocks suggesting that in garnet–whole-rock systems the closure temperature of Lu–Hf is greater than or equal to that of Sm–Nd [28].

Tie lines joining garnet and corresponding whole rock for the low-temperature peridotites have positive slopes (Fig. 4), a feature consistent with Hf isotope re-equilibration in the garnet–whole-rock system. In contrast, the tie lines joining garnet–whole-rock pairs for the high-temperature samples (except porphyroclastic peridotite NK1-7) have negative (or flat) slopes, which could reflect recent Hf infiltration (Fig. 4). The fact that the whole-rock Hf isotope compositions of the high-temperature xenoliths plot close to that of the Nikos kimberlite is consistent with an interpretation that these peridotites experienced Hf addition during sample transport.

5.4. Evolution of Archean lithosphere

The Hf isotopic composition of lithospheric mantle underlying Archean cratons has yet to be clearly established because of former difficulties with the analytical method prior to the development of MC-ICP-MS. Recent investigations have focused on Hf and Nd isotopic determinations for 3.8 Ga old supracrustal rocks from the Isua province of Greenland in order to characterize the isotopic composition of the early terrestrial mantle [46,47]. These samples exhibit a significant range in both initial Hf and Nd isotope ratios, which are dominantly more radiogenic than those of chondrites, suggestive of derivation from 'depleted' mantle. The Lu/Hf and Sm/Nd ratios observed in these early Archean rocks, however, are distinct from those inferred for a 'depleted' mantle reservoir [46–48], which as for most terrestrial rocks has been characterized by the covariant evolution of Hf and Nd isotopes [25,49,50]. This relationship has been interpreted to reflect the similar fractionation of Lu and Hf, and Sm and Nd during melt extraction from garnet-free residual peridotite assemblages [25,49,51]. In contrast, melting of mantle peridotite in the presence of garnet (i.e. depths >80 km) results in a significant fractionation of Lu/Hf and Sm/Nd ratios as garnet preferentially incorporates Lu relative to Hf, to a greater extent than Sm relative to Nd [24,46]. The data obtained from the 3.8 Ga old Isua samples suggest that elemental fractionation during partial melting in the early Archean mantle was much stronger than in the post-Archean 'depleted' mantle reservoir and most likely occurred in the presence of garnet [46–48].

A number of the low-temperature Nikos peridotites, which represent the shallow lithosphere beneath the Canadian craton, are characterized by Hf isotopic signatures that are significantly higher compared to that estimated for 'depleted' mantle [40,46]. These xenoliths exhibit superchondritic $^{176}Lu/^{177}Hf$ ratios (Figs. 2b, 3), indicative of strong fractionation of the Lu/Hf ratios during generation of the melt-depleted peridotites. The results can be interpreted as evidence that garnet was present as a residual phase during partial melting and that the Somerset lithosphere stabilized at a minimum depth of 80 km. Over billions of years, these fractionated $^{176}Lu/^{177}Hf$ ratios resulted in the very radiogenic $^{176}Hf/^{177}Hf$ compositions recorded by the low-temperature Nikos peridotites at the time of kimberlite emplacement.

6. Conclusions

The Hf isotopic compositions of the Nikos peridotites indicate significant differences exist between the low-(shallow; $<1100°C$) and high-temperature (deep-seated; $>1100°C$) xenoliths. Although contamination with a kimberlite-related component may have been superimposed on the Hf isotope compositions of a number of xenoliths, it is likely that shallow and deep Somerset lithosphere do not share a common petrogenetic history. The Lu–Hf systematics of the low-temperature Nikos peridotites suggest that the Somerset lithosphere stabilized in the Archean to depths of at least 150 km.

A number of the low-temperature peridotites exhibit superchondritic $^{176}Lu/^{177}Hf$ ratios that suggest mantle root formation in the presence of residual garnet (depths >80 km). These fractionated $^{176}Lu/^{177}Hf$ ratios resulted in the radiogenic $^{176}Hf/^{177}Hf$ signatures observed at the time of kimberlite magmatism. These first Hf isotopic ratios for the subcontinental mantle indicate that at least part of the lithosphere beneath the North American craton is characterized by more radiogenic Hf isotope signatures than estimates for 'depleted' mantle.

Acknowledgements

We thank F. Rasselet for assistance in the field and for handpicking separates of magmatic kimberlite for isotope analysis. S.S. and A.S. are indebted to J. Blichert-Toft for introducing them to the secrets of Lu–Hf chemistry. The MC-ICP-MS facility is supported by a MFA grant from NSERC and the research was funded by a NSERC operating grant to D.F. Francis. S.S. is grateful for financial support in the form of a NSERC doctoral scholarship. The manuscript was greatly improved by comments from the reviewers, J. Blichert-Toft, J. Vervoort, and G. Nowell, and feedback from Alex Halliday.*[AH]*

References

[1] T.H. Jordan, Structure and formation of the continental tectosphere, J. Petrol., Special Lithosphere Issue (1988) 11–37.
[2] S.P. Grand, Mantle shear structure beneath the Americas and surrounding oceans, J. Geophys. Res. 99 (1994) 11591–11621.
[3] F.R. Boyd, S.A. Mertzman, Composition and structure of the Kaapvaal lithosphere, southern Africa, in: B.O. Mysen (Ed.), Magmatic Processes: Physiochemical Principles, Geol. Soc. Spec. Publ. 1 (1987) 13–24.
[4] P.H. Nixon, Kimberlitic xenoliths and their cratonic setting, in: P.H. Nixon (Ed.), Mantle Xenoliths, John Wiley, Chichester, 1987, pp. 215–239.
[5] W.F. McDonough, Constraints on the composition of the continental lithospheric mantle, Earth Planet. Sci. Lett. 101 (1990) 1–18.
[6] T.H. Jordan, Mineralogies, densities and seismic velocities of garnet lherzolites and their geophysical implications, in: F.R. Boyd, H.O.A. Meyer (Eds.), The Mantle Sample: Inclusions in Kimberlites and Other Volcanics, American Geophysical Union, Washington, DC, 1979, pp. 1–13.
[7] H.N. Pollack, Cratonization and thermal evolution of the mantle, Earth Planet. Sci. Lett. 80 (1986) 175–182.
[8] A. Zindler, S. Hart, Chemical geodynamics, Annu. Rev. Earth Planet. Sci. 14 (1986) 493–571.
[9] A.J. Erlank, F.G. Waters, C.J. Hawkesworth, S.E. Haggerty, H.L. Allsopp, R.S. Rickard, M.A. Menzies, Evidence for mantle metasomatism in peridotite nodules from the Kimberley pipes, South Africa, in: M.A. Menzies, C.J. Hawkesworth (Eds.), Mantle Metasomatism, Academic Press, London, 1987, pp. 221–311.
[10] M.A. Menzies, Archean, Proterozoic, and Phanerozoic

lithospheres, in: M.A. Menzies (Ed.), Continental Mantle, Oxford University Press, Oxford, 1990, pp. 67–86.
[11] C. Brooks, D.E. James, S.R. Hart, Ancient lithosphere: its role in young continental volcanism, Science 139 (1976) 1086–1094.
[12] D.G. Pearson, The age of continental roots, Lithos 48 (1999) 171–194.
[13] G.M. Yaxley, A.J. Crawford, D.H. Green, Evidence for carbonatite metasomatism in spinel peridotite xenoliths from western Victoria, Earth Planet. Sci. Lett. 107 (1991) 305–317.
[14] R.L. Rudnick, W.F. McDonough, B.W. Chappell, Carbonatite metasomatism in the northern Tanzanian mantle, Earth Planet. Sci. Lett. 114 (1993) 463–475.
[15] R.W. Carlson, A.J. Irving, Depletion and enrichment history of subcontinental lithospheric mantle: Os, Sr, Nd and Pb evidence for xenoliths from the Wyoming Craton, Earth Planet. Sci. Lett. 126 (1994) 457–472.
[16] D.G. Pearson, R.W. Carlson, S.B. Shirey, F.R. Boyd, P.H. Nixon, Stabilisation of Archean lithospheric mantle: a Re-Os isotope study of peridotite xenoliths from the Kaapvaal craton, Earth Planet. Sci. Lett. 134 (1995) 341–357.
[17] D.G. Pearson, S.B. Shirey, R.W. Carlson, F.R. Boyd, N.P. Pokhilenko, N. Shimizu, Re-Os, Sm-Nd, and Rb-Sr isotope evidence for thick Archean lithospheric mantle beneath the Siberian craton modified by multistage metasomatism, Geochim. Cosmochim. Acta 59 (1995) 959–977.
[18] G.J. Irvine, M.G. Kopylova, R.W. Carlson, D.G. Pearson, S.B. Shirey, B.A. Kjarsgaard, Age of the lithospheric mantle beneath and around the Slave craton: a Rhenium-Osmium isotopic study of peridotite xenoliths from the Jericho and Somerset Island kimberlites, Ninth Annual V.M. Goldschmidt Conference, LPI Contrib. 971 (1999) 134–135.
[19] J. Dalmasso, G. Barci-Funel, G.J. Ardisson, Reinvestigation of the decay of the long-lived odd-odd ^{176}Lu nucleus, Appl. Radiat. Isot. 43 (1992) 69–76.
[20] Y. Nir-El, N. Lavi, Measurement of half-life of ^{176}Lu, Appl. Radiat. Isot. 49 (1998) 1653–1655.
[21] J. Blichert-Toft, C. Chauvel, F. Albarède, Separation of Hf and Lu for high-precision isotope analysis of rock samples by magnetic sector-multiple collector ICP-MS, Contrib. Mineral. Petrol. 127 (1997) 248–260.
[22] R.M. Bedini, J.-L. Bodinier, Distribution of incompatible trace elements between the constituents of spinel peridotite xenoliths: ICP-MS data from the East African Rift, Geochim. Cosmochim. Acta 63 (1999) 3883–3900.
[23] S.R. Hart, T. Dunn, Experimental clinopyroxene-melt partitioning of 24 trace elements, Contrib. Mineral. Petrol. 113 (1993) 1–8.
[24] H. Fujimaki, M. Tatsumoto, K.I. Aoki, Partition coefficients of Hf, Zr, and REE between phenocrysts and groundmasses, J. Geophys. Res. 89 (1984) B662–B672.
[25] P.J. Patchett, M. Tatsumoto, Hafnium isotope variations in oceanic basalts, Geophys. Res. Lett. 7 (1980) 1077–1080.
[26] P.J. Patchett, M. Tatsumoto, Lu–Hf total-rock isochron for the eucrite meteorites, Nature 288 (1980) 571–574.
[27] S. Duchêne, J. Blichert-Toft, B. Luais, P. Télouk, J.-M. Lardeaux, F. Albarède, The Lu–Hf dating of garnets and the ages of the Alpine high-pressure metamorphism, Nature 387 (1997) 586–589.
[28] E.E. Scherer, K.L. Cameron, J. Blichert-Toft, Lu–Hf garnet geochronology: Closure temperature relative to the Sm–Nd system and the effects of trace mineral inclusions, Geochim. Cosmochim. Acta 64 (2000) 3413–3432.
[29] S.S. Schmidberger, D. Francis, Nature of the mantle roots beneath the North American craton mantle xenolith evidence from Somerset Island kimberlites, Lithos 48 (1999) 195–216.
[30] J. Pell, New kimberlite discoveries on Somerset Island, in: Exploration Overview 1993, Yellowknife, NWT Geology Division, Department of Indian and Northern Affairs, 1993, 47 pp.
[31] L.H. Heaman, The nature of the subcontinental mantle from Sr-Nd-Pb isotopic studies on kimberlite perovskite, Earth Planet. Sci. Lett. 92 (1989) 323–334.
[32] C.B. Smith, H.L. Allsopp, O.G. Garvie, J.D. Kramers, P.F.S. Jackson, C.R. Clement, Note on the U-Pb perovskite method for dating kimberlites: examples from the Wesselton and DeBeers mines, South Africa, and Somerset Island, Canada, Chem. Geol. (Isot. Geosci.) 79 (1989) 137–145.
[33] T. Frisch, P.A. Hunt, Reconnaissance U-Pb geochronology of the crystalline core of the Boothia Uplift, District of Franklin, Northwest Territories, in: Radiogenic Age and Isotope Studies: Report 7, Geological Survey of Canada, Paper 93-2, 1993, pp. 3–22.
[34] W.F. McDonough, S.S. Sun, The composition of the earth, Chem. Geol. 120 (1995) 223–253.
[35] S.S. Schmidberger, D. Francis, Constraints on the trace element composition of the Archean mantle root beneath Somerset Island, Arctic Canada, J. Petrol. 42 (2001) 1095–1117.
[36] S.S. Schmidberger, A. Simonetti, D. Francis, Sr-Nd-Pb isotope systematics of mantle xenoliths from Somerset Island kimberlites: Evidence for lithosphere stratification beneath Arctic Canada, Geochim. Cosmochim. Acta 65 (2001) 4243–4255.
[37] N. Machado, A. Simonetti, U-Pb dating and the Hf isotope composition of zircon by laser-ablation-MC-ICP-MS, in: Laser-ablation-ICPMS in the Earth Sciences, Mineralogical Association of Canada, Short Course 29, 2001, pp. 121–146.
[38] W.A. Russell, D.A. Papanastassiou, T.A. Tombrello, Ca isotope fractionation on the Earth and other solar system materials, Geochim. Cosmochim. Acta 42 (1978) 1075–1090.
[39] S.S. Schmidberger, E. Hegner, Geochemistry and isotope systematics of calc-alkaline volcanic rocks from the Saar-Nahe basin (SW Germany) – implications for Late-Varis-

can orogenic development, Contrib. Mineral. Petrol. 135 (1999) 373–385.
[40] J. Blichert-Toft, F. Albarède, The Lu–Hf isotope geochemistry of chondrites and the evolution of the mantle–crust system, Earth Planet. Sci. Lett. 148 (1997) 243–258.
[41] J.B. Dawson, A review of the geology of kimberlite, in: P.J. Wyllie (Ed.), Ultramafic and Related Rocks, Wiley, New York, 1967, pp. 241–251.
[42] C.B. Smith, Pb, Sr and Nd isotopic evidence for sources of southern African Cretaceous kimberlites, Nature 304 (1983) 51–54.
[43] G.M. Nowell, D.G. Pearson, P.D. Kempton, S.R. Noble, C.B. Smith, Origins of kimberlites: a Hf isotope perspective, in: Proceedings of the Seventh International Kimberlite Conference, 1999, pp. 616–624.
[44] J.D. Vervoort, P.J. Patchett, F. Albarède, J. Blichert-Toft, R. Rudnick, H. Downes, Hf-Nd isotopic evolution of the lower crust, Earth Planet. Sci. Lett. 181 (2000) 115–129.
[45] J.A. Dalton, D.C. Presnall, The continuum of primary carbonatitic-kimberlitic melt compositions in equilibrium with lherzolite: data from the system CaO-MgO-Al_2O_3-SiO_2-CO_2 at 6 GPa, J. Petrol. 39 (1998) 1953–1964.
[46] J.D. Vervoort, J. Blichert-Toft, Evolution of the depleted mantle: Hf isotope evidence from juvenile rocks through time, Geochim. Cosmochim. Acta 63 (1999) 533–556.
[47] J. Blichert-Toft, F. Albarède, M. Rosing, R. Frei, D. Bridgwater, The Nd and Hf isotopic evolution of the mantle through the Archean. Results from the Isua supracrustals, West Greenland, and from the Birimian terranes of West Africa, Geochim. Cosmochim. Acta 63 (1999) 3901–3914.
[48] F. Albarède, J. Blichert-Toft, J.D. Vervoort, J.D. Gleason, M. Rosing, Hf-Nd isotope evidence for a transient dynamic regime in the early terrestrial mantle, Nature 404 (2000) 488–490.
[49] P.J. Patchett, Hafnium isotope results from mid-ocean ridges and Kerguelen, Lithos 16 (1983) 47–51.
[50] J.D. Vervoort, P.J. Patchett, J. Blichert-Toft, F. Albarède, Relationships between Lu–Hf and Sm–Nd isotopic systems in the global sedimentary system, Earth Planet. Sci. Lett. 168 (1999) 79–99.
[51] C.M. Johnson, B.L. Beard, Evidence from hafnium isotopes for ancient sub-oceanic mantle beneath the Rio Grande rift, Nature 362 (1993) 441–444.
[52] W.D. Steward, Late Proterozoic to Early Tertiary stratigraphy of Somerset Island and northern Boothia Peninsula, District of Franklin, Geological Survey of Canada, Paper 83-26, 1987, 78 pp.